Stem Cell Reports
Resource
ISSCR
OPEN ACCESS

Generation of a TPH2-EGFP reporter cell line for purification and monitoring of human serotonin neurons *in vitro* and *in vivo*

Ting Xu,[1] Jinjin Duan,[1,2] Yingqi Li,[1] Guanhao Wang,[1] Shuanqing Li,[1] You Li,[1] Wenting Lu,[1] Xinyi Yan,[1] Yixuan Ren,[1] Fei Guo,[3] Lining Cao,[1,*] and Jianfeng Lu[1,4,*]

[1]Shanghai YangZhi Rehabilitation Hospital (Shanghai Sunshine Rehabilitation Center), Frontier Science Center for Stem Cell Research, School of Life Sciences and Technology, Tongji University, Shanghai 200092, China
[2]School of Life Sciences, Shanghai University, Shanghai 200444, China
[3]Key Laboratory of Receptor Research, Shanghai Institute of Materia Medica, Chinese Academy of Sciences, Shanghai 201203, China
[4]Suzhou Institute of Tongji University, Suzhou 215101, China
*Correspondence: crystalvivining@aliyun.com (L.C.), lu.jianfeng@tongji.edu.cn or healthygod_world@hotmail.com (J.L.)
https://doi.org/10.1016/j.stemcr.2022.08.012

SUMMARY

Generation of serotonin neurons (SNs) from human pluripotent stem cells (hPSCs) provides a promising platform to explore the mechanisms of serotonin-associated neuropsychiatric disorders. However, neural differentiation always yields heterogeneous cell populations, making it difficult to identify and purify SNs *in vitro* or track them *in vivo* following transplantation. Herein, we generated a TPH2-EGFP reporter hPSC line with insertion of *EGFP* into the endogenous tryptophan hydroxylase 2 (*TPH2*) locus using CRISPR-Cas9-mediated gene editing technology. This TPH2-reporter, which faithfully indicated TPH2 expression during differentiation, enabled us to obtain purified SNs for subsequent transcriptional analysis and study of pharmacological responses to antidepressants. In addition, the reporter system showed strong EGFP expression to indicate SNs, which enabled us to explore *in vitro* and *ex vivo* electrophysiological properties of SNs. In conclusion, this TPH2-EGFP reporter cell line might be of great significance for studies on human SN-related development and differentiation, drug screening, disease modeling, and cell replacement therapies.

INTRODUCTION

Serotonin (5-hydroxytryptamine or 5-HT), a well-known monoamine neurotransmitter, has been implicated in a wide variety of physiological functions and behaviors, including emotional regulation, autonomic regulation, circadian rhythmicity, breathing, eating, and sleep. Although more than 90% of the total body serotonin is found in the peripheral organs, more attention has been directed toward its function in the CNS. Serotonin plays important roles in regulating CNS development and function (Keszthelyi et al., 2009). It has been reported that serotonergic dysregulation is involved in the pathogenesis of many psychiatric disorders (including major depression disorder, anxiety disorders, eating disorders, schizophrenia, and aggressive behaviors) and neurological disorders (including locomotor dysfunction following spinal cord injury [SCI], chronic neuropathic pain, autism, migraine, and seizures) (Ghosh and Pearse, 2014; Hamel, 2007; Muller et al., 2016; Nordquist and Oreland, 2010; Richerson and Buchanan, 2011; Wei et al., 2010). However, the exact involvement of serotonin neurons (SNs) in these neuropsychiatric disorders is still unclear.

Human pluripotent stem cells (hPSCs)-derived SNs can be used for disease modeling and drug screening, and it helps to elucidate the etiology of serotonin-associated diseases and develop more promising therapies for treating them. In recent years, several attempts have been made to obtain SNs from hPSCs by manipulating signaling pathways (Lu et al., 2016; Valiulahi et al., 2021). However, due to the nature of heterogeneous differentiation, *in vitro* differentiation often yields low purity of SNs and other uncharacterized cell types in the heterogeneous cell populations, making it difficult to detect the functions of live SNs, to monitor their activities in a real-time manner, or to compare the molecular changes between wild-type (WT) and mutated human SNs.

Biosynthesis of brain serotonin depends on its rate-limiting biosynthetic enzyme: tryptophan hydroxylase 2 (TPH2), which is preferentially expressed by the SNs in human brain (Walther et al., 2003). TPH2 is thus one of the most frequently used markers for identifying SNs. Therefore, generating a TPH2-reporter cell line will be helpful to identify and purify hPSCs-derived SNs from a mixed cell population or to track SNs in a real-time manner. Recently, several efforts had been attempted to establish reporter cell lines by placing a reporter gene into *Tph2* gene locus of mouse cell lines; however, one of the reporter cell lines was not fully characterized, and the gene editing efficiency was very low (Migliarini et al., 2013; Pacini et al., 2017); another engineered reporter cell line even could not produce detectable reporter-TPH2 fusion protein (Menzorov et al., 2019). Considering the extensive differences in serotonin signaling between human and mouse (Hodge et al., 2019), it is necessary to establish a system to report human SNs for accurate and careful investigation. Vadodaria et al. tried to label human fibroblast-derived SNs, but the reporter gene expression was mediated by lentivirus-based

random integration instead of precise genome editing technique, thus leading to unfaithful labeling of SNs (Vadodaria et al., 2016).

In this regard, using CRISPR-Cas9-mediated gene editing technology, we established a highly efficient approach to generate a stable TPH2-enhanced green fluorescent protein (EGFP) reporter hPSC line with insertion of *EGFP* gene before the stop codon of the endogenous human *TPH2* locus. The reporter cell line maintained the pluripotency and was capable of differentiating into SNs with EGFP labeling, which enabled us to identify and purify SNs from heterogeneous cell populations *in vitro*. The purified SNs showed more accurate pharmacological responses to three types of antidepressants, indicating its value in drug screening. The transcriptome profiling of the reporter cell line at the three key stages during SN differentiation confirmed the identity of SNs and revealed the expression profiles of purified mature SNs. The EGFP-expressing neurons also displayed SN-specific electrophysiological properties. For *in vivo* study, the reporter cell line-derived serotonergic neural progenitors (SNPs) were transplanted into the dorsal raphe nuclei (DRN)-lesioned mice. These cells survived and integrated into the host DRN; more excitingly, the grafted human cells displayed remarkable EGFP fluorescence under the control of *TPH2* promoter, which enabled us to perform electrophysiological analysis for transplanted SNs *in vivo*.

In conclusion, the TPH2-reporter hPSC line may provide a valuable tool for understanding the role of SNs in neurological disorders, for drug screening to assess the 5-HT-depleting and 5-HT-releasing reagents, and for SN-based cell therapies.

RESULTS

Selection of targeting vector

To generate a TPH2-reporter cell line, the reporter cassette (T2A-EGFP-CMV-Puro) was inserted before the stop codon of *TPH2* gene. In order to increase the success rate of knockin, two single guide RNAs (sgRNAs) (sgRNA1 and sgRNA2) were designed and compared. The target sequence, a 20-nt sequence on *TPH2* gene locus complementary to sgRNA, is shown in Figures 1A and 1B. It is worth noting that the sgRNA/Cas9 complex could recognize the target sequence and keep cutting the DNA when the 20-nt target sequence and PAM remain intact (Jiang and Doudna, 2017). As shown in Figure 1A, the sequence of Target 1 and PAM was located on the left homology arm (HAL) of donor plasmid and remained intact after homologous recombination (HR)-mediated knockin, thus allowing Cas9 to recognize and cut the donor plasmid and the edited gene locus after homology-directed repair (HDR). To avoid the undesired cutting on the donor vector or HDR-edited gene locus, the sequence of Target 2 and PAM was designed to span the HAL and right homology arm (HAR) of the donor vector, of which neither HAL nor HAR contained the intact sequence of Target 2 and PAM (Figure 1B). Consequently, the CRISPR target site would be disrupted once the reporter cassette was inserted into the intended position (Figure 1B). The candidate targeting vector sgRNA1-Cas9 or sgRNA2-Cas9 in combination with the donor vector were electroporated into hPSCs (H9, a human embryonic stem cell line) respectively. After puromycin selection and PCR screening, Sanger sequencing was performed on the selected clones to evaluate the editing efficiency of the two sgRNAs. Sequencing analysis revealed the presence of indels at cleavage site targeted by sgRNA1/Cas9 (Figure 1C) but not in sgRNA2/Cas9-mediated editing (Figure 1D). Indeed, sgRNA1/Cas9 would theoretically keep cutting the HDR-edited gene locus until the cell introduces indels or the wrong nucleotides, which could disrupt the intact sequence of Target 1 and PAM. Then the frequency of indel events that occurred in the two groups was evaluated. After puromycin selection, several clones were randomly selected from the edited cells of the two groups respectively. As shown in Figure 1E, 11 out of 14 selected clones transfected with sgRNA1/Cas9 showed indels, whereas none of the 16 selected clones transfected with sgRNA2/Cas9 showed indels. This result indicated that the sgRNA1/Cas9-mediated cutting on the target site after repair might introduce unexpected indels and substantially decrease the efficiency of gene editing. Based on this, sgRNA2/Cas9 was selected as the targeting vector in this study.

Generation of TPH2-EGFP reporter hPSC line

The targeting vector sgRNA2/Cas9 and the donor vector TPH2-T2A-EGFP were electroporated into hPSCs (H9) to generate TPH2-EGFP reporter cell line. After 48 h of recovery, cells were positively selected by puromycin. 1 week later, individual puromycin-resistant clones were picked up and screened by PCR. Briefly, the PCR screening was performed with three primer sets (Figures 2A–2C, upper panel): 5TP and 3TP primer sets, which spanned the nucleotide outside of the homologous arm to the internal reporter/selection cassette, were designed to test if the insertion cassette was integrated into the expected gene locus; TN primer set, which flanked about 500 bp of the stop codon of WT *TPH2* gene, was designed to determine homozygous or heterozygous clones. As shown in Figures 2A–2C, clones (1, 3, 4, 5, 6, 8, 9, 10, 11, 12, 13, 14, 16) showed the 1,600-bp band (PCR product amplified using 5TP primer pair, Figure 2A) and the 2,000-bp band (PCR product amplified using 3TP primer pair, Figure 2B), indicating in-frame integration of the reporter cassette into the *TPH2*

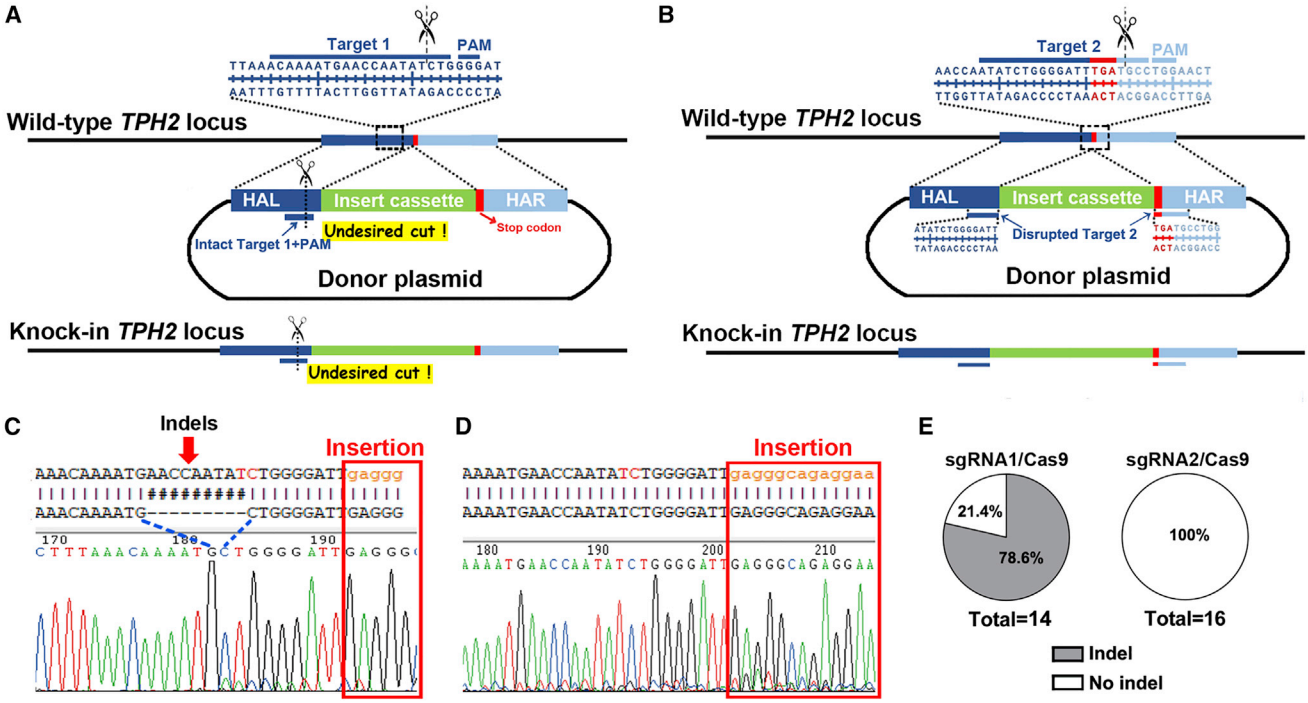

Figure 1. Schematic diagram of CRISPR-Cas9-mediated integration of reporter cassette into human *TPH2* locus and design of sgRNAs

(A) Schematic diagram of sgRNA1/Cas9-mediated undesired cutting on donor plasmid and HDR-edited gene locus. Target 1 (dark-blue bar) is the target sequence complementary to sgRNA1. The full sequence of Target 1 and PAM is in HAL (dark blue). The full sequence (Target 1 + PAM), which keeps intact in donor plasmid and knockin *TPH2* locus, can be targeted and cut by sgRNA1/Cas9 complex. The Cas9 cleavage sites are indicated by black scissors. Red bar: stop codon; light blue bar: HAR.

(B) Schematic diagram for strategy to avoid CRISPR-Cas9-mediated undesired cutting on donor plasmid and knockin *TPH2* locus. Target 2 (a bar with mixed color: dark blue, red, and light blue) is the target sequence complementary to sgRNA2. The total sequence of Target 2 and PAM is disrupted by insert cassette in donor plasmid and HDR-edited *TPH2* locus, so it cannot be recognized and cut by sgRNA2/Cas9. Red bar: stop codon; light blue bar: HAR.

(C) The sequencing result of the engineered clones guided by sgRNA1. (D) The sequencing result of engineered clones guided by sgRNA2.

(E) The frequency of indel formation. (HDR, homology directed repair; HAL, left homology arm; HAR, right homology arm).

locus. Heterozygous targeted clones showed 500-bp band, whereas clone 11 lacked the WT band, indicating homozygous integration of the TPH2 reporter cassette (Figure 2C). In order to evaluate the efficiency and the reproducibility of this gene editing system, the reporter cassette was inserted into the *TPH2* locus of another human embryonic stem cell line (H1) and a human induced PSC (iPSC) line (ZSSY001) respectively. We then performed genotype screening on them. As shown in Figures 2A–2C, S1, and Table S1, a high targeting rate was achieved in the selected clones: the efficiency of heterozygous and homozygous knockin is up to 77% and 12%, respectively. The top 10 potential off-target sites (Table S2) were evaluated in the homozygous reporter lines (H9-Clone#11, H1-Clone#11, iPSC-Clone#10) by Sanger sequencing. No indel formation was detected in these sites (Figures S2A), suggesting the high specificity of this gene editing system. The copy number of the inserted EGFP in the homozygote reporter cell line (H9-Clone#11) was determined by quantitative genotyping PCR (qgPCR) (Figures S2A and S2B). According to the PCR fluorescence data-derived linear regression equation (Figure S2C) and SAS system-based statistical analysis (Yuan et al., 2007), the copy number of the inserted EGFP gene was proved to be equal with the copy number of the endogenous *TPH2* gene (ratio = 1.138789, Figure S2D). Therefore, the *EGFP* gene was inserted as a single copy at the *TPH2* locus of the reporter cell line. The homozygote reporter cell line (H9-Clone#11) was then selected for the entire study unless specially indicated. To identify any possible indels and confirm in-frame integration of the reporter cassette, Sanger sequencing was performed to detect the positive PCR products. Sanger sequencing results confirmed the 5′-end junction (Figure 2D, Site 1), the T2A-EGFP junction (Figure 2D, Site 2), and the 3′-end junction (Figure 2D, Site 3) between the original *TPH2* DNA sequence and the inserted sequence, and no indels were

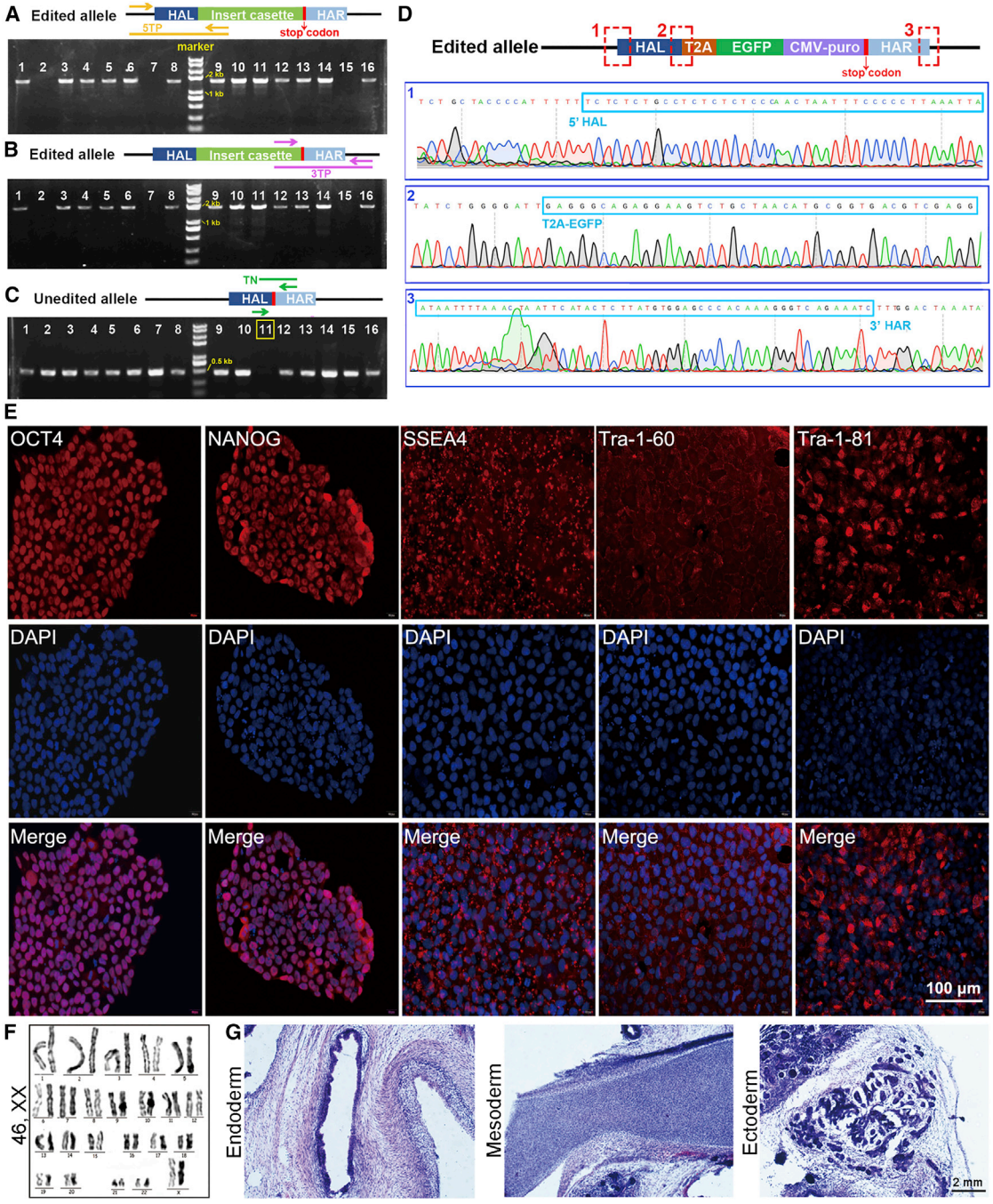

Figure 2. Establishment of the TPH2-reporter cell line

(A) Genotyping of the modified H9 clones with the primer set 5TP to identify the targeted allele, in which the product is detected as a 1600-bp band (DNA marker was given in the middle lane indicating the size of PCR amplicons).

(B) Genotyping of the modified H9 clones with the primer set 3TP to identify the targeted allele, in which the product is detected as a 2000-bp band.

(C) Genotyping of the modified H9 clones with the primer set TN to determine homozygous (no band) or heterozygous clones (a 500-bp band).

(D) Representative Sanger sequencing chromatograms for the homozygous Clone#11 of H9.

(E) Immunofluorescence analysis of the TPH2-EGFP reporter cell line (H9-Clone#11) for pluripotency markers (OCT4, NANOG, SSEA4, Tra-1-60, Tra-1-81). Scale bar, 100 μm.

(legend continued on next page)

detected. These data indicated that T2A-EGFP-CMV-puro cassette was correctly inserted into *TPH2* gene locus with high efficiency and specificity.

Then the pluripotency of the reporter hPSC line was evaluated. The reporter cell line expressed pluripotent markers, such as OCT4 and NANOG in the nuclei, and SSEA4, Tra-1-60, and Tra-1-81 on the cell membrane (Figure 2E). Karyotyping was also detected in the reporter hPSC line and found to be normal (Figure 2F). The teratoma formation assay showed the engineered cells could be differentiated into cells of three germ layers (Figure 2G). This result suggested that the TPH2-EGFP reporter hPSC line maintained the normal karyotype and pluripotency after gene editing and puromycin selection.

Verification of TPH2 reporter activity during SN differentiation *in vitro*

In order to confirm the reporter activity of the engineered cells, TPH2-EGFP reporter cells were differentiated into SNs according to our established protocol (Lu et al., 2016) (Figure 3A). Co-activation of WNT and SHH signal pathways prompted the reporter cells to program into SNPs expressing NKX2.2, FOXA2, SOX1, and GATA2 (Figure 3B for H9-Clone#11). After an additional 2–4 weeks of neuronal differentiation, the neurons showed typical serotonergic markers, such as TPH2, 5-HT, and GATA-3′ (Figure 3C for H9-Clone#11, Figure S3A for H1-Clone#11, and Figure S3B for iPSC-Clone#10). The engineered reporter cell line (H9-Clone#11) showed similar differentiation potential with the parental cell line (Figures S4A and S4B), indicating that the gene editing did not affect the differentiation potential of the cells.

The EGFP labeling enabled us to isolate and purify SNs from the heterogeneous cell populations by fluorescence-activated cell sorting (FACS) (Figure 3D). The sorted cells were seeded on poly-*l*-ornithine (PO)/laminin-coated coverslips for about 2 days, and then they displayed a healthy status and elongated nerve fibers, which is a unique character of neuronal growth (Figure 3E). After reseeding, the purified neurons rapidly formed neural network within 1 week (Figure S4C). TPH2 was specifically expressed in the sorted EGFP-positive population, but not in the EGFP-negative population (Figure 3E). More importantly, the percentage of TPH2+ cells (95.43% ± 1.032%, n = 3) in the purified population was significantly higher than that (22.08% ± 7.584%, n = 3) in the mixed cell population (Figure 3F). This result showed that TPH2-EGFP reporter could faithfully indicate SNs and enable us to purify SNs from heterogeneous differentiation cultures *in vitro*.

Transcriptional profiles of reporter cells during differentiation toward SNs

In order to profile the transcriptional alterations of the reporter cells during differentiation toward SNs, we performed RNA-seq analysis at the three key stages of differentiation: the initial stage of differentiation (hPSCs/Day0, TPH2 not expressed), SNPs (Day21, TPH2 not expressed), and the purified SNs after FACS (Day42, TPH2+/GFP+ cells) (Figure 4A). The samples were remarkably divided into three populations based on the principal component analysis (PCA) (Figure 4B). Hierarchical clustering of the gene expression patterns exposed that the SNs had distinctly different transcriptional profiles compared with SNPs and hPSCs (Figure 4C). In order to verify the identity of SNs, the interested genes were selected for heatmap analysis. The pluripotency markers were highly expressed at Day0, and ventral and hindbrain markers were highly expressed at Day21, whereas serotonergic markers (*SLC18A2*, *GATA3*, *GATA2*, *MAO-B*, *FEV*, *TPH2*, and *DDC*) were highly expressed at Day42. Moreover, genes coding neuropeptides (*CRH* and *TAC1*), neuropeptide receptors (*OXTR* and *INSR*), and proteolytic enzymes of neuropeptides (*CPE* and *PCSK1*) were highly expressed in SNs (Day42), indicating that many neuropeptides and transmitters may be co-localized in SNs together with 5-HT (Figure 4D). Then Short Time-Series Expression Miner (STEM) analysis was performed to determine the overall trends of gene expression changes during the three stages. We found the trend curves of the gene signatures clustered in profile 13 were all gradually upregulated during the whole stages of SNs differentiation (Figure 4E). Kyoto Encyclopedia of Genes and Genomes pathway (KEGG) enrichment analysis was performed to identify functional categories of the upregulated genes in profile 13. It showed that the cluster of genes was enriched in "vasopressin-regulated water reabsorption" (Figure 4F). Differentially expressed genes (DE-Gs) analysis showed that thousands of genes differentially expressed among the three groups (Figure 4G). The 1,095 (869 + 226) upregulated genes (Figure 4H), which were shared by both groups (Day0 and Day21) compared with cells at SNs stage (Day42), were selected to evaluate the expression profiles of transcription factors (TFs). Krüppel-like factor (KLF) family members and activating transcription factor 3 (*ATF3*), which have been shown to promote axon regeneration (Cooke et al., 2022), were upregulated in the purified SNs (Figure 4I). The 869 genes, which were exclusively upregulated in SNs stage (Day42) (Figure 4H), were selected for functional analysis. The GO enrichment analysis showed that four biological functional regions

(F) Karyotyping analysis of the TPH2-EGFP reporter cell line (H9-Clone#11).
(G) H&E staining for the TPH2-EGFP reporter cell line (H9-Clone#11)-derived teratoma. Scale bar, 2 mm.
See also Figures S1 and S2, Tables S1 and S2.

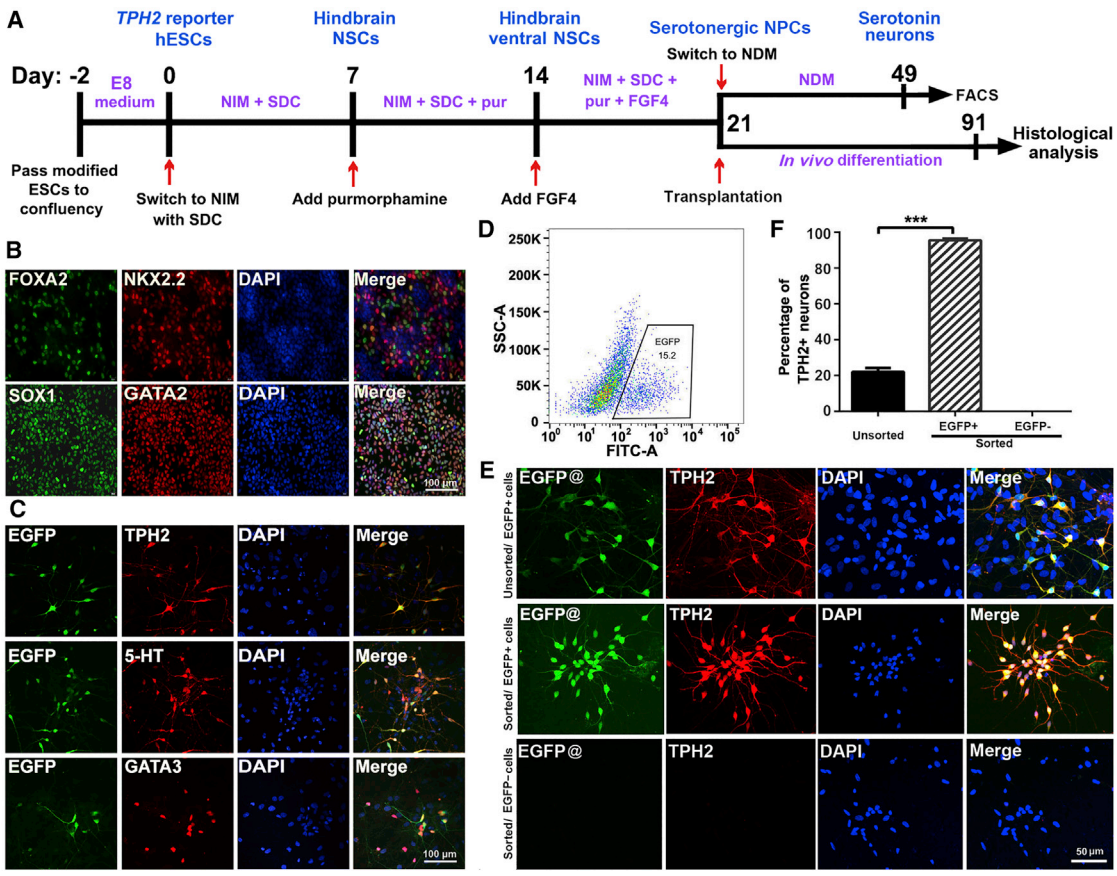

Figure 3. Verification of TPH2 reporter activity during serotonin neurons (SNs) differentiation *in vitro*

(A) Schematic diagram of the strategy to generate SNs from the TPH2 reporter hPSCs.

(B) Representative images of immunofluorescence staining with NKX2.2, FOXA2, GATA2, and SOX1 in reporter cell (H9-Clone#11)-derived serotonergic neural progenitors (SNPs). Scale bar, 100 μm.

(C) Representative images of immunofluorescence staining with 5-HT, GATA3, and TPH2 in reporter cell (H9-Clone#11)-derived mature SNs. Scale bar, 100 μm.

(D) FACS profile of TPH2-EGFP reporter cell (H9-Clone#11)-derived SNs.

(E) Immunostaining of TPH2 in the sorted or unsored neurons. Scale bar, 50 μm.

(F) The percentage of SNs determined by the number of TPH2+ cells over the total cells (DAPI+) in sorted or unsorted cells. (Unsorted n = 3, sorted n = 3, "n" refers to independent experiments, ***p < 0.001).

Error bars represent SEM; SDC: SB431542, DMH1, CHIR99021; pur, purmorphamine; NDM, neural differentiation medium; NIM, neural induction medium; NSCs, neural stem cells; NPCs, neural progenitor cells; EGFP@, staining with EGFP antibody.

See also Figures S3 and S4.

(axon, synapse, neuron projection, nervous system development) were significantly enriched (Figure 4J), indicating the neuronal identity of SNs. In addition, KEGG showed that three biological functional regions (serotonergic synapse, dopaminergic synapse, glutamatergic synapse) were enriched (Figure 4K), which confirmed the SN identity and raised the possibility that SNs might be involved in the action of dopaminergic and glutamatergic systems. Interestingly, Substance P (SubP), a neuropeptide encoded by *TAC1* gene and reported to be primarily expressed by SNs in the mouse caudal medullary raphe nuclei (Okaty et al., 2015), was expressed in about 30% of the rostral human SNs within mixed population (Figures 4L and 4M). These data suggested that the transcriptome profiling of the reporter cell line at the three key stages during SNs differentiation confirmed the identity of SNs and revealed the expression profiles of purified mature SNs.

Functional analysis of TPH2-EGFP reporter SNs *in vitro*

Application of stem cells for drug screening is hindered due to the lack of consistent differentiation efficiency with high purity of specific neurons (Inoue et al., 2014). To

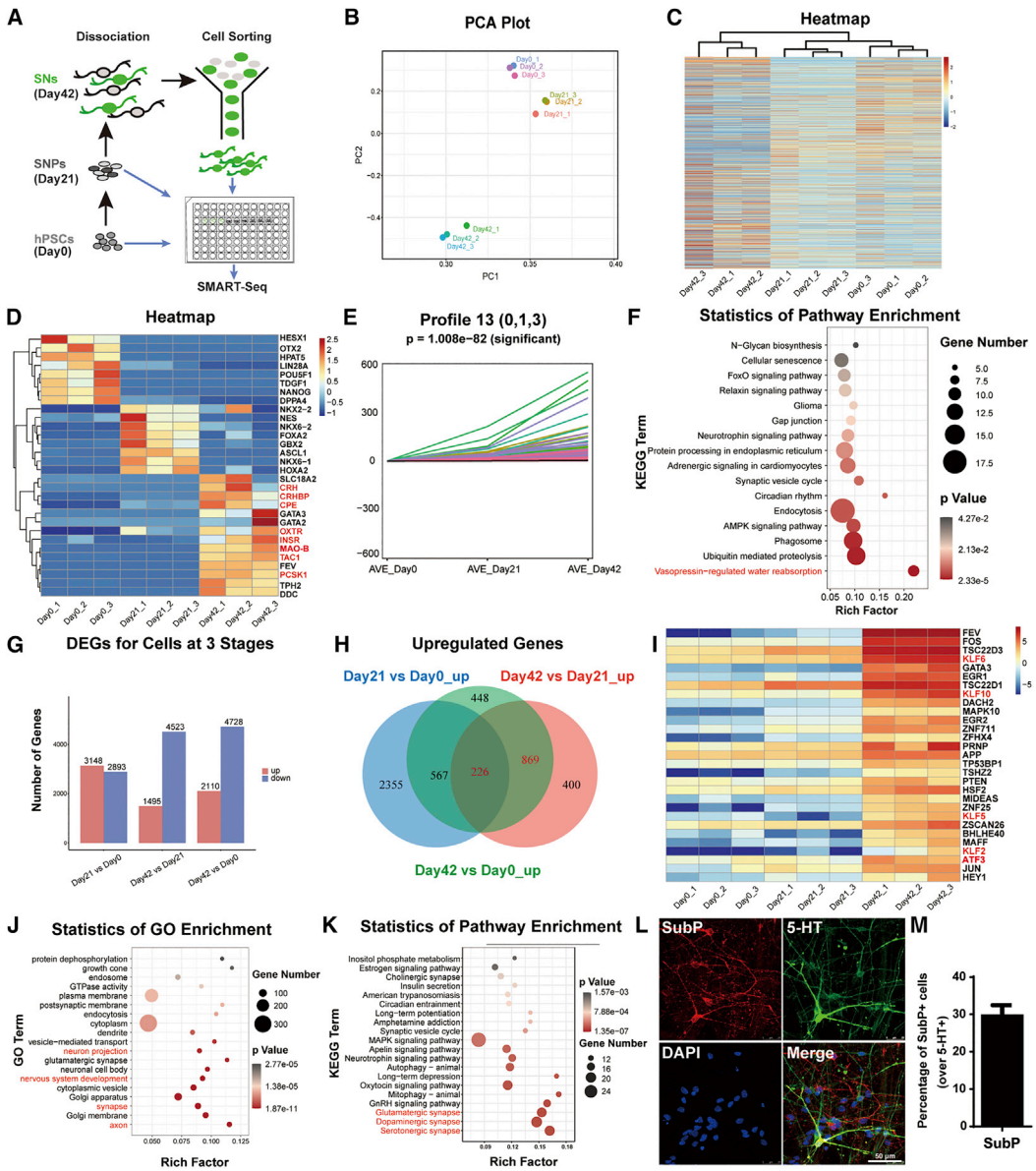

Figure 4. Transcriptome analysis of TPH2-reporter cells during the differentiation toward SNs

(A) The schematic of sample collection from three stages of SNs differentiation (Day0: hPSCs stage; Day21: SNPs stage; Day42: EGFP+ mature SNs stage) and SMART-Seq.

(B) Principal component analysis (PCA).

(C) Hierarchical clustering analysis.

(D) Heatmap of the interested gene expression profile.

(E) Short Time-Series Expression Miner (STEM) analysis.

(F) Scatterplot of KEGG pathway enrichment analysis of the interested genes from STEM analysis.

(G) Differentially expressed genes (DE-Gs) analysis.

(H) The Venn diagram for the upregulated genes.

(I) Heatmap of expression profiling of upregulated transcription factors (TFs).

(J and K) Scatterplot of GO and KEGG pathway enrichment analysis of the overlapped upregulated genes.

(L) Immunostaining of SubP for the mature SNs (Day42). Scale bar, 50 μm.

(M) is quantification for (L), n = 4 independent experiments. SubP: substance P.

overcome this issue, we utilized the TPH2-EGFP reporter system to obtain SNs with 95% purity (Figure 3F). At day 42 of differentiation (stage of SNs), we confirmed that the 5-HT production from TPH2 reporter SNs (Edited) was similar to that from the parent H9 cells-derived SNs (WT) (Figure 5A), indicating that gene editing did not affect the function of SNs to secrete neurotransmitter. Then three types of antidepressants were chosen to treat the unsorted or purified SNs to induce 5-HT secretion: amitriptyline (APL) is a tricyclic antidepressant (TCA), phenelzine sulfate (PLZ) is a nonselective monoamine oxidase (MAO) inhibitor (MAOI), and escitalopram oxalate (EO) is a selective serotonin reuptake inhibitor (SSRI). We found that treatment with PLZ or EO significantly increased 5-HT secretion by SNs in both unsorted cell populations and purified SNs. However, it is to be noticed that APL treatment did not show significant effect on promoting 5-HT secretion in unsorted cell populations, while this effect was obviously shown in purified SNs (Figures 5B and 5C). In order to compare the sensitivity to antidepressants between unsorted and purified SNs, alteration ratios of extracellular 5-HT levels after the treatment of antidepressants were applied. Because of the significant batch variation in unsorted SNs, no statistically significant difference of alteration ratios could be observed among the three antidepressants, although the changes were obvious (Figure 5D). When the alteration ratios in the culture of purified SNs were analyzed, a very clear difference of sensitivity to antidepressants was shown with statistical significance (Figure 5E). This demonstrated that the highly purified SNs with consistent quality offered an attractive and reliable drug screening tool for antidepressants.

Given that the reporter hPSC-derived EGFP+ neurons expressed typical serotonergic markers, we next investigated the electrophysiological properties of these EGFP+ neurons. Before recording, the reporter neurons could be visualized under the fluorescence microscope by expressing the fluorescent protein EGFP (Figure 5F). Whole-cell patch-clamp recordings were performed on the EGFP+ neurons after 5 weeks of culture in neuron differentiation medium (NDM). The mean input resistance (R_{in}) was 639.1 ± 87.3 MΩ (n = 7). Inward Na^+ and outward K^+ currents were observed with a 40-ms voltage step (–40 mV to +30 mV) (Figures 5G–5I), indicating that the physiological function of Na^+/K^+ channels in the EGFP+ SNs was normal, thus providing a physiological basis for the generation of action potentials. Indeed, whole-cell patch-clamp recording method could induce the EGFP+SNs to generate action potentials by injecting step currents (Figures 5J and 5K), and the release frequency was positively correlated with the intensity of the injected currents. In addition, these EGFP+ cells could generate low frequency (2.3 ± 0.4 Hz) of spontaneous action potentials and spontaneous excitatory postsynaptic currents (EPSCs) (Figures 5L and 5M), which are consistent with the electrophysiological features of SNs derived from non-edited hPSCs (Lu et al., 2016).

Tracking transplanted human SNs *in vivo*

In order to examine whether TPH2-EGFP reporter could indicate TPH2 expression *in vivo* and be used for cell tracking after transplantation, DRN lesion was performed as we previously described (Cao et al., 2020). 4 weeks after lesion surgery, TPH2-EGFP reporter hPSC-derived SNPs were transplanted into the DRN of the DRN-lesioned SCID mice (Figure S5). 10 weeks after transplantation, the transplanted human cells survived and grafted into the host DRN area. For EGFP+ cells, around 96% of them were TPH2+ (Figures 6A–A″, arrowhead, and Figure S6A), and about 92% of them were 5-HT+ (Figures 6B–6B″, arrowhead, and Figure S6A), suggesting that EGFP reporter could faithfully indicate TPH2 expression *in vivo*. These TPH2/EGFP (Figures 6A–A″, arrowhead) or 5-HT/EGFP (Figures 6B–B″, arrowhead) double-positive cells also displayed typical neuronal morphology with branching dendrites and axons, suggesting that the transplanted SNPs survived very well and differentiated into SNs. The EGFP+ cells were double-stained with human nuclei (HuN, a human-specific nuclear marker) (Figures 6C–C″, arrowhead), indicating that the EGFP+ cells were of human origin. About 4% of HuN+ cells were labeled with EGFP, suggesting that these grafted human cells differentiated into SNs *in vivo* (Figure S6B). We then investigated the migration capacity of the transplanted cells by histological analysis of the sagittal brain sections. Most of the EGFP+/5-HT+ cells localized in the DRN area (the injection site, Figure 6D, inset 1, and Figure 6E), and a few EGFP+/5-HT+ cells migrated to the cerebellum (Figure 6D, inset 2, and Figure 6E), medulla (Figure 6D, inset 3, and Figure 6G), hypothalamus (Figure 6D, insets 4 and 5, and Figures 6H and 6I), and pons (Figure 6D, inset 6, and Figure 6J), sprouting branching outgrowth and acquiring neuron-like morphology. This result indicated that TPH2-EGFP reporter could be applied for tracking the transplanted human SNs, which may facilitate the detection of human SNs *in vivo*.

Functional integration of reporter cell line-derived SNs in the mouse brain

Finally, we evaluated the functionality of reporter cell line-derived SNs integrated into the mouse DRN, using whole-cell patch-clamp recordings of EGFP+ SNs on *ex vivo* brain slices obtained from the mice 10 weeks after transplantation (Figure 7A). The average R_{in} of the EGFP+ neurons (n = 12) was 788.6 ± 98.2 MΩ. In voltage-clamp configuration, characteristic inward Na^+ and outward K^+ currents were evoked by 40-ms voltage stepped from −40 mV to +30 mV (Figures 7B–7D), suggesting that the Na^+/K^+ channels were

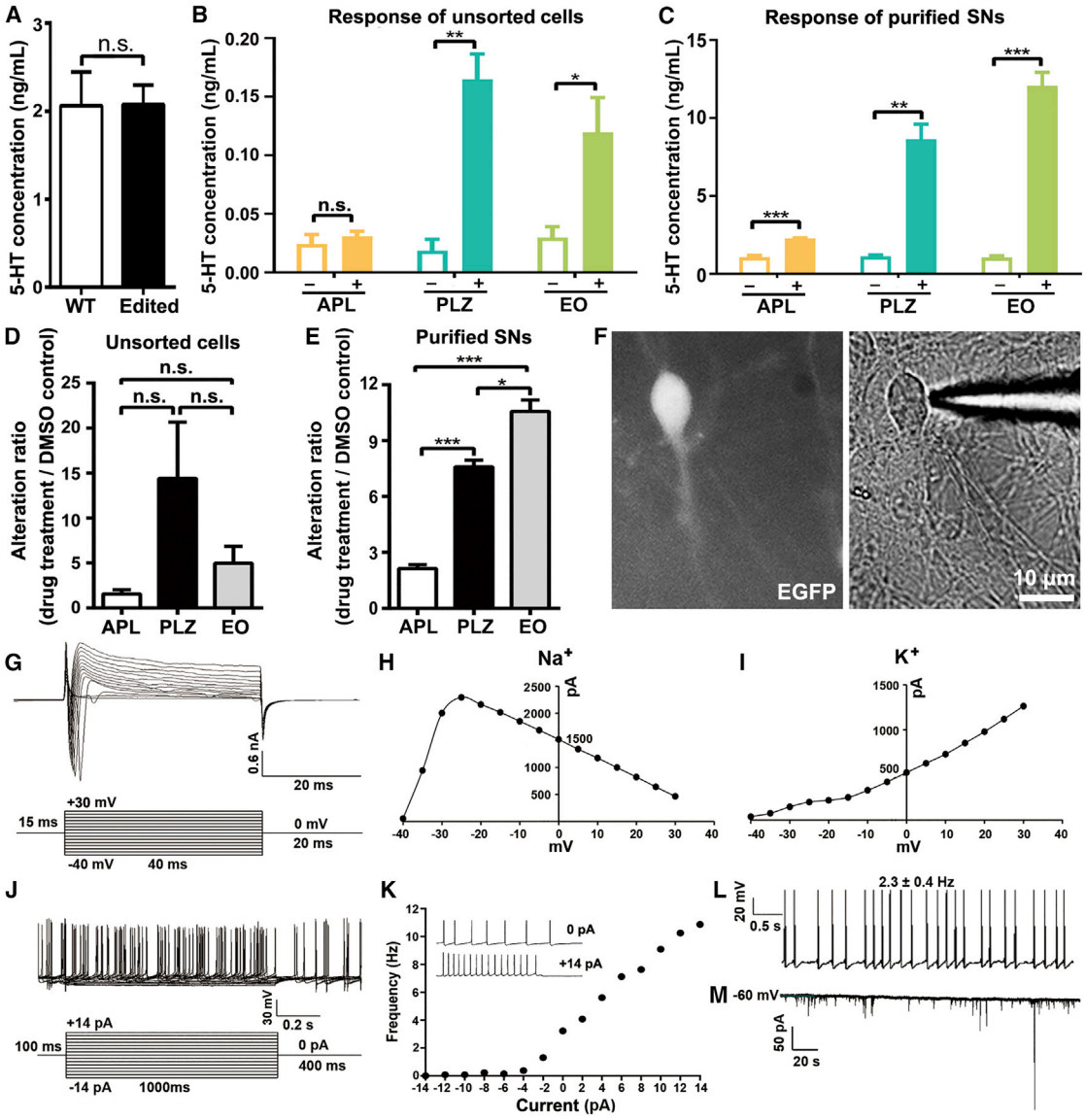

Figure 5. Functional analysis of the TPH2-EGFP reporter SNs *in vitro*

(A) Comparison of 5-HT secretion between WT cells (H9) and edited reporter cells (H9-Clone#11) (both in unsorted situation).

(B) Extracellular 5-HT released by unsorted mixed cells before and after treatment with antidepressants.

(C) Extracellular 5-HT released by sorted purified EGFP+ cells before and after treatment with antidepressants.

(D–E) Evaluation of the sensitivity to antidepressants of mixed (D) or purified (E) SNs.

(F) Representative bright field and fluorescent images of TPH2-reporter SNs patched by the micropipette electrode for whole-cell patch-clamp recording. Scale bar, 10 μm.

(G) Current traces evoked by 40-ms depolarizing voltage stepped from −40 to +30 mV in 5-mV increments and input voltage program (protocol).

(H–I) Current-voltage curves for voltage-gated Na^+ (H) and K^+ (I) currents (n = 6).

(J) Program of input current (protocol) and schematic diagram of action potentials induced by current stimulation.

(K) Action potentials triggered by input current from −14 pA to +14 pA; (n = 6).

(L) Representative trace of spontaneous action potentials; (n = 3).

(M) Representative trace of spontaneous excitatory postsynaptic potential (EPSC) release. Statistical significance p values were determined using t tests (*$p < 0.05$; **$p < 0.01$; ***$p < 0.001$; n.s.: no significance).

For data in (A–E), n = 3 independent experiments. For data in (G–M), "n" refers to the number of recorded cells, and the experiments were performed for at least three times with different batches of cells. All data are presented as means ± SEM. APL, amitriptyline; PLZ, phenelzine sulfate; EO, escitalopram oxalate.

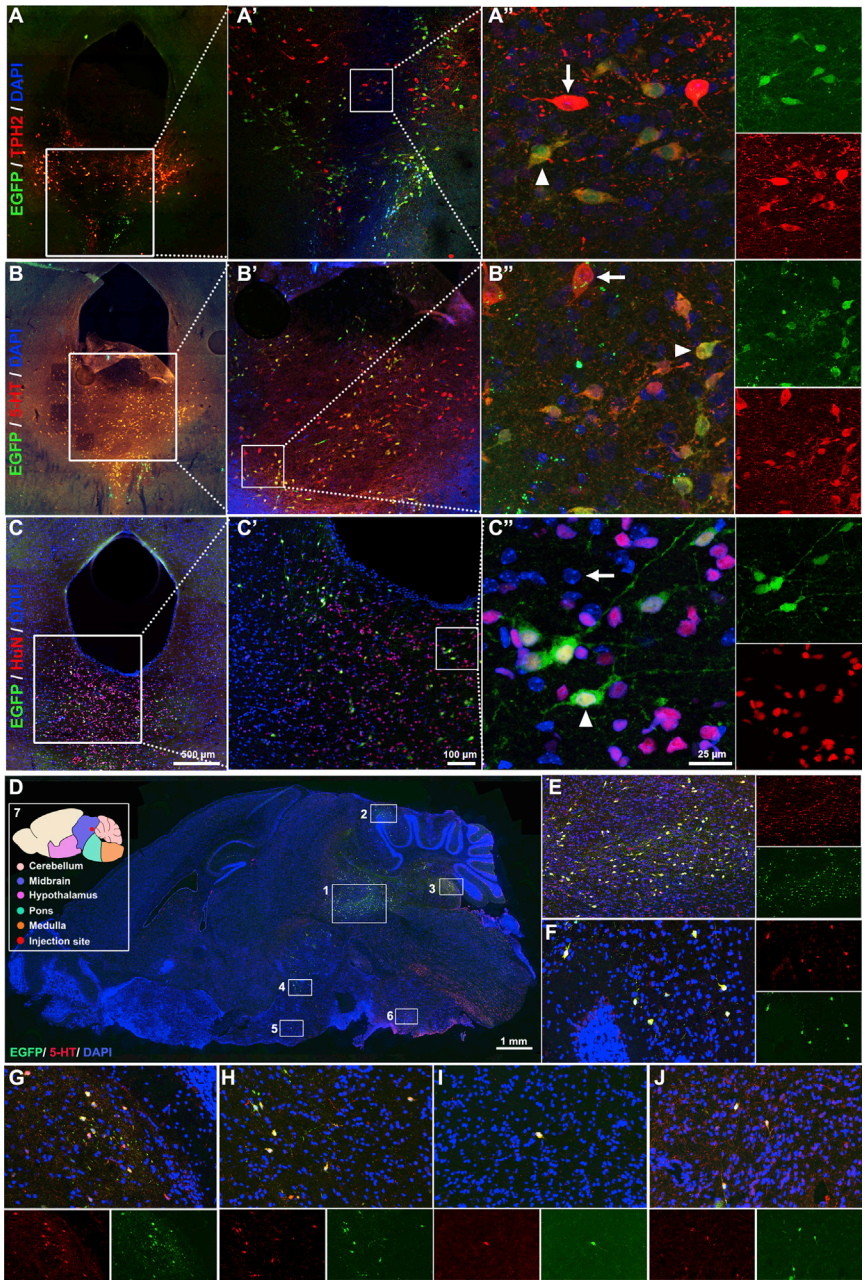

Figure 6. Tracking transplanted human SNs *in vivo*

(A–C) Immunofluorescence staining of SN-specific markers TPH2 (A, A′, A″) and 5-HT (B, B′, B″), and the specific marker for human cells, human nuclei (HuN) (C, C′, C″) of mouse brain coronal sections 10 weeks following transplantation. All cells are nuclear counterstained with DAPI (blue). A, B, C: the general view of dorsal raphe (DR) coronal sections. Scale bar, 500 μm. A′, B′, C′: the enlarged images of the white insets in A, B, C. Scale bar, 100 μm. A″, B″, C″: the enlarged images of the white insets in A′, B′, C′. Scale bar, 25 μm. Arrowheads in A″, B″, C″ indicate transplanted mature SNs, while arrows in A″ and B′ indicate endogenous mouse SNs, and the arrow in C″ indicates endogenous mouse cell nucleus.

(D) Immunofluorescence staining of SN-specific marker 5-HT (red) of mouse brain sagittal sections 10 weeks following transplantation. Scale bar, 1 mm. (Inset 7: the schematic of the injection and migration sites on the sagittal brain section).

(E–J) The enlarged views of inset 1–6 shown in (D) respectively.

See also Figures S5 and S6.

physiologically functional for the grafted neurons to generate action potentials. Indeed, the frequency of action potentials increased as the intensity of the stimulus (current injections) was increased (Figures 7E and 7F). In addition, the grafted neuron displayed spontaneous action potentials (Figure 7G). The synaptic properties of grafted human cells were also evaluated. In acute slices, five of nine EGFP+ neurons exhibited spontaneous EPSCs at −60 mV in voltage-clamp mode (Figure 7H), indicating that the grafted human neurons had functional postsynaptic machinery to receive excitatory synaptic inputs from nearby neurons. Taken together, these data showed that the grafted human cells were able to display stereotypical neuronal electrophysiological characteristics, such as firing properties and excitatory synaptic activity, indicating their ability to integrate into the host brain neural circuits.

DISCUSSION

Recently, our group and others have successfully generated human SNs from hPSCs and fibroblasts. However, the

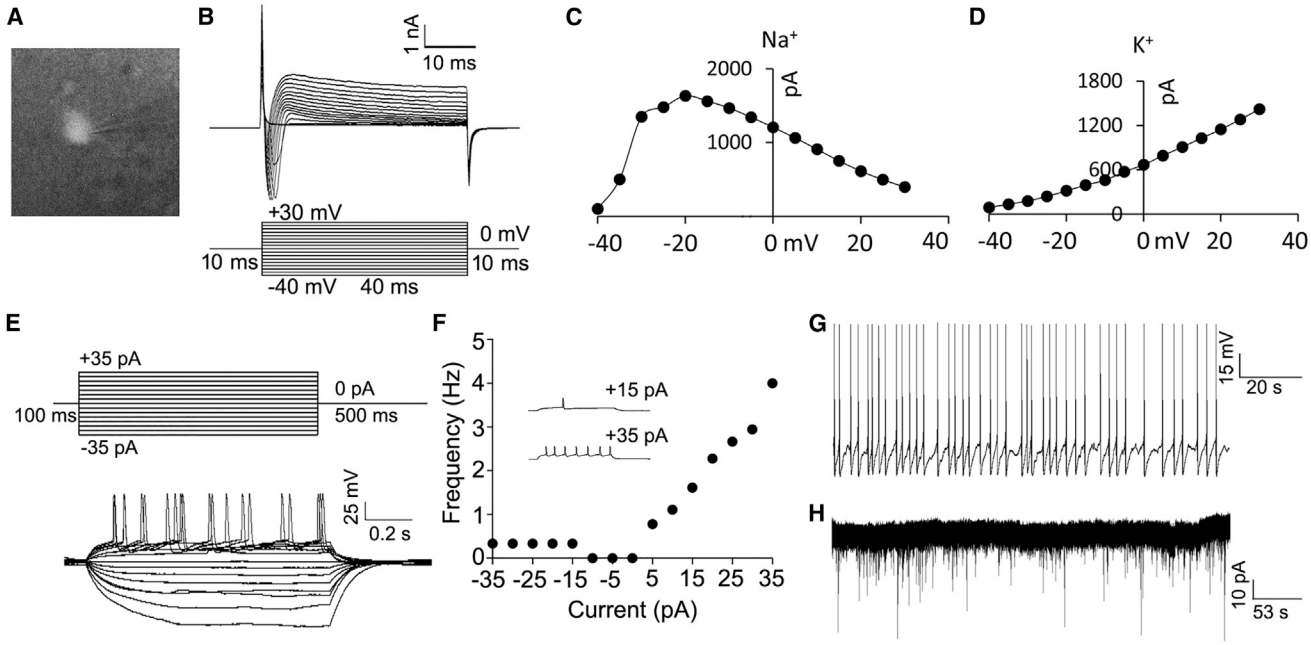

Figure 7. Functional integration of TPH2-EGFP reporter cell line-derived SNs in the mouse brain

(A) Representative fluorescent images of TPH2-reporter SNs patched by the micropipette electrode for whole-cell patch-clamp recording.

(B) Current traces (upper) evoked by 40-ms depolarizing voltage stepped from −40 to +30 mV in 5-mV increments and input voltage program (lower, protocol).

(C and D) Current-voltage curves for voltage-gated Na^+ (C) and K^+ (D) currents; (n = 11).

(E) Input current program (upper, protocol) and action potentials evoked by current steps from −35 to +35 pA in 5-pA increments (lower).

(F) Action potential frequency induced by injected current; (n = 3).

(G) Representative trace of spontaneous action potentials of the grafted cell recorded in current-clamp configuration at 0 pA.

(H) Representative trace of spontaneous excitatory postsynaptic current (EPSC) recorded in voltage-clamp configuration at −60 mV; "n" refers to the number of recorded cells, and the experiments were performed for at least three times with different batches of cells from different mice.

differentiated progeny is a heterogeneous mixture containing SNs and non-SNs, which makes it difficult to monitor SNs and potentially confounds the related phenotypic analysis both *in vitro* and *in vivo*. TPH2 is a typical marker for identifying SNs, so a TPH2-reporter cell line enables us to identify, purify, and track SNs.

In the present study, we established a highly efficient approach to generate a human TPH2-EGFP reporter cell line with insertion of *EGFP* into the endogenous human *TPH2* locus following the coding sequence through CRISPR-Cas9-mediated HR (Figure 1B). We have achieved a high targeting rate of 89% (77% + 12%) in selected clones (Figures 2A–2C and S1), demonstrating a high efficiency of CRISPR-Cas9-mediated HR. Then the Sanger sequencing confirmed that the T2A-EGFP-CMV-puro cassette was correctly inserted into *TPH2* gene locus (Figure 2D). The TPH2-EGFP reporter hPSC line maintained the normal karyotype (Figure 2F) and pluripotency (Figures 2E and 2G) after gene editing and puromycin selection. A homozygous TPH2-EGFP reporter cell line (H9-Clone#11) was then selected and differentiated into SNs (Figure 3C) with functional electrophysiological properties *in vitro* (Figures 5F–5M), according to our established protocol (Figure 3A) (Lu et al., 2016). The TPH2-EGFP reporter could indicate endogenous *TPH2* gene expression and enabled us to purify SNs (Figures 3D–3F) for subsequent transcriptional analysis (Figure 4) and study of pharmacological responses to antidepressants (Figures 5A–5E). For *in vivo* studies, we found that the reporter hPSC line-derived SNPs survived and grafted into host DRN following transplantation, and finally differentiated into EGFP-labeled mature SNs (Figure 6) with functional electrophysiological properties *in vivo* (Figure 7).

The CRISPR-Cas9 technology has emerged as a versatile tool for gene editing. In the present study, an up to 89% targeting rate was achieved in the selected clones (Figures 2A–2C and S1), indicating a high efficiency of sgRNA2/Cas9-mediated HR. Other groups had previously attempted to generate a Tph2-GFP mouse embryonic stem cell line by replacing 105-nt of *Tph2* gene downstream of the start codon with the reporter-*GFP* gene via

untargeted-HDR strategy; however, only 4 of 96 neomycin-resistant clones (about 4%) had the desired integration within the *Tph2* locus (Migliarini et al., 2013).

One advantage of the current reporter system is that the EGFP expression driven by the *TPH2* promoter faithfully indicated the endogenous TPH2 expression during the *in vitro* and *in vivo* differentiation process. Pacini et al. reported that the transplanted mouse Tph2-GFP reporter cells needed to be stained with anti-GFP antibody to acquire optimal demonstration of GFP (Pacini et al., 2017). Menzorov et al. reported that the expression level of mEos2-Tph2 reporter of mouse embryonic stem cells was too low to produce detectable fluorescent proteins for the neuronal tracing by fluorescent microscopy (Menzorov et al., 2019). Compared with the mouse Tph2 reporter cell lines established by other groups (Menzorov et al., 2019; Migliarini et al., 2013; Pacini et al., 2017), the transplanted TPH2-EGFP reporter cell derived-human SNs displayed direct optimal EGFP fluorescence under fluorescent microscope without extra immunostaining with anti-EGFP antibody (Figure 7A).

Another advantage of this reporter system is that the TPH2-EGFP reporter does not affect the endogenous TPH2 expression and the whole procedure of SNs differentiation. This TPH2 reporter system enables us to purify SNs after TPH2 expression turns on and to explore transcriptome profiles for purified SNs (Figure 4). Previously, studies had been conducted to explore transcriptional profiling of human SNs: (1) Valiulahi et al. generated SNs from hPSCs by activation of Sonic Hedgehog and Retinoic acid signaling and performed transcriptome analysis for SNs (Valiulahi et al., 2021). However, the analysis might be not optimal because the cells used for transcriptome analysis were not purified SNs and might contain multiple lineages. (2) Vadodaria et al. performed whole transcriptome RNA-seq for the human fibroblasts-derived transdifferentiated SNs, which was purified by a lentiviral reporter. But this transcriptome analysis might not be ideal because of two reasons: the accuracy of lentivirus-mediated SN labeling was 70%, whereas the labeling accuracy of our reporter system was more than 90% (Figure S6A), and the serotonergic fate was induced by overexpressing the key TFs for SNs, which might mask the true expression levels of the TFs (Vadodaria et al., 2016). By using the current TPH2-EGFP reporter system, we profiled the whole transcriptome for purified human SNs. Several TFs (KLF family members and *ATF3*), which were reported to promote axon sprouting and regeneration (Cooke et al., 2022), were highly expressed in purified SNs (Figure 4I). This finding may help uncover the mechanism of SN-mediated axon regeneration (Miazga et al., 2018; Hawthorne et al., 2011; Hou et al., 2020; Huang et al., 2021). In addition, we found that SubP was expressed in human rostral SNs (Figures 4L and 4M). This is different from the previous study that suggested that SubP was primarily expressed in mouse caudal SNs (Okaty et al., 2015). The current finding hints an unidentified role of SubP in human rostral SNs.

Stem cell technologies provide a source of human cells that can theoretically be expanded to sufficient quantity for drug screening and toxicology studies. We and others had tried to explore the pharmacological responses of hPSCs-derived SNs to SSRI antidepressants, which indicated human SNs with low purity also showed significantly increased 5-HT secretion when treated with EO (Lu et al., 2016; Valiulahi et al., 2021). However, the disparities in differentiation efficiency and the heterogeneity of cell types in the culture may mask the true pharmacological responses to the antidepressants (Figures 5B and 5D). In this study, we obtained highly enriched SNs with 95% purity by FACS (Figure 3F) and explored their pharmacological responses to three types of antidepressants (Figures 5C and 5E). Compared with unsorted SNs, the purified SNs showed significantly more accurate pharmacological responses to the three types of antidepressants (Figures 5B–5E). To date, no research has been reported to analyze the pharmacological responses of human SNs to TCA and MAOI antidepressants. It is known that TCA and SSRIs inhibit 5-HT reuptake to increase synaptic level of 5-HT by binding to serotonin transporter located presynaptically on serotonergic axon terminals, so it is reasonable that APL and EO induced purified SNs to release higher levels of 5-HT (Figures 5C and 5E). Human genome encodes two isoenzymes of MAO: MAO-A and MAO-B. MAO-A, which is predominantly localized in dopamine neurons, is believed to mediate metabolic degradation of 5-HT, whereas MAO-B, which is predominantly localized in SNs, is believed to mediate the degradation of dopamine (Finberg and Rabey, 2016). Our RNA-seq data also confirmed that purified SNs at day 42 of differentiation predominantly express MAO-B instead of MAO-A (Figure 4D). Theoretically, MAOI may not induce a dramatic increase of extracellular 5-HT level due to the lack of MAO-A in purified SNs. However, surprisingly, when treated with PLZ (a nonselective MAOI), the extracellular 5-HT levels were increased both in the unsorted and purified SNs cultures (Figures 5B and 5C). According to the previous report, MAO-B has low enzymatic activity instead of no enzymatic activity for 5-HT degradation (O'Carroll et al., 1983). Thus, one possible explanation for PLZ-induced strong pharmacological responses might be due to the high concentration of PLZ. However, further study should be conducted to understand why purified SNs showed such strong responses to MAOI. Our TPH2-EGFP report system-based purified SNs will be helpful to uncover the truth.

More excitingly, the TPH2 reporter cells-derived neurons showed typical electrophysiological properties of

functional neurons both *in vitro* and *in vivo*. For *in vitro* studies, the reporter cells-derived SNs displayed normal electrophysiological properties similar to that of non-edited SNs (Lu et al., 2016). Brain slice electrophysiology is a golden standard to evaluate whether the grafted cells can develop physiological properties of mature neurons and functionally integrate into host neural circuitry. Although powerful, this technology has its limitations due to the difficulty in identifying the grafted specific neurons in the brain tissue. Generation of a stable reporter to indicate SNs makes it possible to evaluate the functional integration of the grafted SNs (Figure 7). Recently, SN-based cell replacement therapy received lots of attention as a potential novel treatment for SCI. In 2018, Miazga et al. found that intraspinal grafting of SN-enriched rodent embryonic caudal brainstem could improve the locomotor recovery in the grafted SCI rats via regulating expressions of *Htr2a* and *Htr7* (Miazga et al., 2018). In 2020, Hou et al. reported that transplantation of SN-enriched rodent embryonic raphe nucleus-derived cells into SCI rats could improve SCI-induced cardiovascular function by reconstitution of serotonergic regulation on sympathetic activity (Hou et al., 2020). Although implantation of SN-enriched embryonic brain tissue can attenuate above complications following SCI in rodents, a reliable donor cell source is required for accurate investigation. Especially, functional electrophysiological study on grafted SNs will no doubt help demonstrate the reconstruction of neural circuitry formed by grafted SNs and the host tissues. Fortunately, the current reporter cell line-derived SNPs could differentiate into mature SNs with direct remarkable EGFP fluorescence *in vivo* (Figure 7A), which enabled us to perform *ex vivo* brain slice electrophysiology to analyze the functional integration of the grafted cells. Therefore, our established TPH2-EGFP reporter cell line might be a valuable tool for tracking the grafted SNs *in vivo*, promoting the development of SN-based cell replacement therapy.

Taken together, we successfully established an approach to generate a TPH2 reporter hPSC line that faithfully indicated endogenous *TPH2* gene expression during *in vitro* and *in vivo* differentiation process. This might be of great significance in studies of SN development and differentiation, drug screening, disease modeling, and SN-based cell therapies.

EXPERIMENTAL PROCEDURES

Detailed methods are provided in the supplemental experimental procedures.

Design of sgRNA and construction of targeting vectors

The sgRNA was designed using the Benchling CRISPR Design Tool (https://www.benchling.com/crispr/) as described elsewhere (Ran et al., 2013). Briefly, the 200-bp regions flanking the stop codon of the *TPH2* gene were analyzed to identify appropriate targeting sites, and two optimal pairs of sgRNA were selected with comprehensive consideration of target score, off-target score, and distance between the Cas9 cutting site and the insertion site. The sgRNA oligos were ordered from Genewiz (Suzhou, China). Then the two pairs of sgRNA (sgT1 and sgT2) oligos were annealed and ligated into plasmid PX330 (Addgene #42230) containing the SpCas9 and the sgRNA scaffold to form two candidate targeting vectors (sgT1-Cas9 and sgT2-Cas9) respectively. The sequences of sgT1 and sgT2 are listed in Table S3.

Serotonin neuron differentiation

TPH2-reporter hPSCs were differentiated into SNs as we previously described with modifications (Lu et al., 2016). Briefly, cells were seeded on Matrigel-coated plates containing TeSR-E8 medium (E8 medium) at $5 \times 10^4/cm^2$ density. When the cells reached 80% confluence, the E8 medium was changed to neural induction medium (NIM) containing DMEM/F12: Neurobasal (1:1), 1 × N2, 1 × B27, 1 × NEAA, 1 × GlutaMAX, 1.4 μM CHIR99021, 2 μM SB431542, 2 μM DMH1 for 1 week and then passaged. Cells were then treated with 0.5 μM purmorphamine in NIM for another week. During the third week, 10 ng/mL FGF4 was added to the culture medium. On day 21, cells were dissociated by TrypLE and counted. 10,000 cells per cover slip were seeded onto PO/laminin-coated coverslips and treated with NDM containing Neurobasal, 1 × N2, 1 × B27, 1 × NEAA, 0.2 mM vitamin C, 2.5 μM DAPT, 10 ng/mL GDNF, 10 ng/mL BDNF, 1 ng/mL TGFβ3, and 10 ng/mL IGF1 for 2 to 5 weeks. Detailed information for reagents is listed in Table S4.

Statistical analysis

Statistical analysis was performed using GraphPad PRISM 6 (GraphPad Software, San Diego, CA, USA). Unpaired Student's t test was used to compare the difference between two groups. All data are expressed as the mean ± the SEM. *$p < 0.05$, **$p < 0.01$, and ***$p < 0.001$ were considered to be significant.

DATA AND CODE AVAILABILITY

RNA-seq data have been deposited in the Gene Expression Omnibus (GEO) database. The accession number for the RNA-seq data reported in this paper is GEO: GSE206341.

SUPPLEMENTAL INFORMATION

Supplemental information can be found online at https://doi.org/10.1016/j.stemcr.2022.08.012.

AUTHOR CONTRIBUTIONS

T.X. planned and performed molecular and cellular experiments, analyzed data, produced the figures, and wrote the manuscript. J.D. and F.G. performed electrophysiological experiments and analysis. Y.L., G.W., S.L., Y.L., W.L., X.Y., and Y.R. performed molecular experiments and collected the data. L.C. performed transplantation-associated experiments, produced the figures, wrote the manuscript, and provided financial support. J.L. designed and

conceived this project, provided financial support, wrote the manuscript, and approved the manuscript.

ACKNOWLEDGMENTS

This work was supported by the National Key Research and Development Program of China (Grant numbers 2021YFA1101300 and 2017YFA0104100); the National Natural Science Foundation of China (Grant numbers 31771644, 81801331, and 31930068); and the Fundamental Research Funds for the Central Universities.

CONFLICT OF INTERESTS

The authors declare no competing interests.

Received: January 28, 2022
Revised: August 24, 2022
Accepted: August 25, 2022
Published: September 22, 2022

REFERENCES

Cao, L., Zhang, Z., Lu, X., Wang, G., Meng, D., Liu, C., Yun, J., Xu, T., Zhao, C., and Lu, J. (2020). Elimination of serotonergic neurons by stereotaxic injection of 5, 7-Dihydroxytryptamine in the dorsal raphe nuclei of mice. J. Vis. Exp. https://doi.org/10.3791/60968.

Cooke, P., Janowitz, H., and Dougherty, S.E. (2022). Neuronal redevelopment and the regeneration of neuromodulatory axons in the adult mammalian central nervous system. Front. Cell. Neurosci. *16*, 872501. https://doi.org/10.3389/fncel.2022.872501.

Finberg, J.P.M., and Rabey, J.M. (2016). Inhibitors of MAO-A and MAO-B in psychiatry and neurology. Front. Pharmacol. *7*, 340. https://doi.org/10.3389/fphar.2016.00340.

Ghosh, M., and Pearse, D.D. (2014). The role of the serotonergic system in locomotor recovery after spinal cord injury. Front. Neural. Circuits *8*, 151. https://doi.org/10.3389/fncir.2014.00151.

Hamel, E. (2007). Serotonin and migraine: biology and clinical implications. Cephalalgia *27*, 1293–1300. https://doi.org/10.1111/j.1468-2982.2007.01476.x.

Hawthorne, A.L., Hu, H., Kundu, B., Steinmetz, M.P., Wylie, C.J., Deneris, E.S., and Silver, J. (2011). The unusual response of serotonergic neurons after CNS Injury: lack of axonal dieback and enhanced sprouting within the inhibitory environment of the glial scar. J. Neurosci. *31*, 5605–5616. https://doi.org/10.1523/JNEUROSCI.6663-10.2011.

Hodge, R.D., Bakken, T.E., Miller, J.A., Smith, K.A., Barkan, E.R., Graybuck, L.T., Close, J.L., Long, B., Johansen, N., Penn, O., et al. (2019). Conserved cell types with divergent features in human versus mouse cortex. Nature *573*, 61–68. https://doi.org/10.1038/s41586-019-1506-7.

Hou, S., Saltos, T.M., Mironets, E., Trueblood, C.T., Connors, T.M., and Tom, V.J. (2020). Grafting embryonic raphe neurons reestablishes serotonergic regulation of sympathetic activity to improve cardiovascular function after spinal cord injury. J. Neurosci. *40*, 1248–1264. https://doi.org/10.1523/JNEUROSCI.1654-19.2019.

Huang, C.X., Zhao, Y., Mao, J., Wang, Z., Xu, L., Cheng, J., Guan, N.N., and Song, J. (2021). An injury-induced serotonergic neuron subpopulation contributes to axon regrowth and function restoration after spinal cord injury in zebrafish. Nat. Commun. *12*, 7093. https://doi.org/10.1038/s41467-021-27419-w.

Inoue, H., Nagata, N., Kurokawa, H., and Yamanaka, S. (2014). iPS cells: a game changer for future medicine. EMBO J. *33*, 409–417. https://doi.org/10.1002/embj.201387098.

Jiang, F., and Doudna, J.A. (2017). CRISPR-Cas9 structures and mechanisms. Annu. Rev. Biophys. *46*, 505–529. https://doi.org/10.1146/annurev-biophys-062215-010822.

Keszthelyi, D., Troost, F.J., and Masclee, A.A.M. (2009). Understanding the role of tryptophan and serotonin metabolism in gastrointestinal function. Neuro Gastroenterol. Motil. *21*, 1239–1249. https://doi.org/10.1111/j.1365-2982.2009.01370.x.

Lu, J., Zhong, X., Liu, H., Hao, L., Huang, C.T.L., Sherafat, M.A., Jones, J., Ayala, M., Li, L., and Zhang, S.C. (2016). Generation of serotonin neurons from human pluripotent stem cells. Nat. Biotechnol. *34*, 89–94. https://doi.org/10.1038/nbt.3435.

Menzorov, A.G., Orishchenko, K.E., Fishman, V.S., Shevtsova, A.A., Mungalov, R.V., Pristyazhnyuk, I.E., Kizilova, E.A., Matveeva, N.M., Alenina, N., Bader, M., et al. (2019). Targeted genomic integration of EGFP under tubulin beta 3 class III promoter and mEos2 under tryptophan hydroxylase 2 promoter does not produce sufficient levels of reporter gene expression. J. Cell. Biochem. *120*, 17208–17218. https://doi.org/10.1002/jcb.28981.

Miazga, K., Fabczak, H., Joachimiak, E., Zawadzka, M., Krzemień-Ojak, Ł., Bekisz, M., Bejrowska, A., Jordan, L.M., and Sławińska, U. (2018). Intraspinal grafting of serotonergic neurons modifies expression of genes important for functional recovery in paraplegic rats. Neural Plast., 4232706. https://doi.org/10.1155/2018/4232706.

Migliarini, S., Pacini, G., Pelosi, B., Lunardi, G., and Pasqualetti, M. (2013). Lack of brain serotonin affects postnatal development and serotonergic neuronal circuitry formation. Mol. Psychiatry *18*, 1106–1118. https://doi.org/10.1038/mp.2012.128.

Muller, C.L., Anacker, A.M.J., and Veenstra-Vanderweele, J. (2016). The serotonin system in autism spectrum disorder: from biomarker to animal models. Neuroscience *321*, 24–41. https://doi.org/10.1016/j.neuroscience.2015.11.010.

Nordquist, N., and Oreland, L. (2010). Serotonin, genetic variability, behaviour, and psychiatric disorders–a review. Ups. J. Med. Sci. *115*, 2–10. https://doi.org/10.3109/03009730903573246.

O'Carroll, A.M., Fowler, C.J., Phillips, J.P., Tobbia, I., and Tipton, K.F. (1983). The deamination of dopamine by human brain monoamine oxidase. Specificity for the two enzyme forms in seven brain regions. Naunyn Schmiedebergs Arch. Pharmacol. *322*, 198–202. https://doi.org/10.1007/BF00500765.

Okaty, B.W., Freret, M.E., Rood, B.D., Brust, R.D., Hennessy, M.L., Debairos, D., Kim, J.C., Cook, M.N., and Dymecki, S.M. (2015). Multi-scale molecular Deconstruction of the serotonin neuron system. Neuron *88*, 774–791. https://doi.org/10.1016/j.neuron.2015.10.007.

Pacini, G., Marino, A., Migliarini, S., Brilli, E., Pelosi, B., Maddaloni, G., Pratelli, M., Pellegrino, M., Ferrari, A., and Pasqualetti, M. (2017). A Tph2 ^{GFP} reporter stem cell line to model in vitro and in vivo serotonergic neuron development and function. ACS

Chem. Neurosci. *8*, 1043–1052. https://doi.org/10.1021/acschemneuro.6b00403.

Ran, F.A., Hsu, P.D., Wright, J., Agarwala, V., Scott, D.A., and Zhang, F. (2013). Genome engineering using the CRISPR-Cas9 system. Nat. Protoc. *8*, 2281–2308. https://doi.org/10.1038/nprot.2013.143.

Richerson, G.B., and Buchanan, G.F. (2011). The serotonin axis: shared mechanisms in seizures, depression, and SUDEP. Epilepsia *52*, 28–38. https://doi.org/10.1111/j.1528-1167.2010.02908.x.

Vadodaria, K.C., Mertens, J., Paquola, A., Bardy, C., Li, X., Jappelli, R., Fung, L., Marchetto, M.C., Hamm, M., Gorris, M., et al. (2016). Generation of functional human serotonergic neurons from fibroblasts. Mol. Psychiatry *21*, 49–61. https://doi.org/10.1038/mp.2015.161.

Valiulahi, P., Vidyawan, V., Puspita, L., Oh, Y., Juwono, V.B., Sittipo, P., Friedlander, G., Yahalomi, D., Sohn, J.W., Lee, Y.K., et al. (2021). Generation of caudal-type serotonin neurons and hindbrain-fate organoids from hPSCs. Stem Cell Rep. *16*, 1938–1952. https://doi.org/10.1016/j.stemcr.2021.06.006.

Walther, D.J., Peter, J.U., Bashammakh, S., Hörtnagl, H., Voits, M., Fink, H., and Bader, M. (2003). Synthesis of serotonin by a second tryptophan hydroxylase isoform. Science *299*, 76. https://doi.org/10.1126/science.1078197.

Wei, F., Dubner, R., Zou, S., Ren, K., Bai, G., Wei, D., and Guo, W. (2010). Molecular depletion of descending serotonin unmasks its novel facilitatory role in the development of persistent pain. J. Neurosci. *30*, 8624–8636. https://doi.org/10.1523/JNEUROSCI.5389-09.2010.

Yuan, J.S., Burris, J., Stewart, N.R., Mentewab, A., and Stewart, C.N. (2007). Statistical tools for transgene copy number estimation based on real-time PCR. BMC Bioinf. *8*, S6. https://doi.org/10.1186/1471-2105-8-S7-S6.